γ-ray bundles at the cores of extensive air showers and primary cosmic ray identification

C. R. A. Augusto, C. E. Navia, and F. A. Pinto
Instituto de Física, Universidade Federal Fluminense, 24210-130, Niterói, Rio de Janeiro, Brazil

S. L. C Barroso and E. H. Shibuya
Instituto de Física, Universidade Estadual de Campinas, 13081-970, Campinas, São Paulo, Brazil

M. Luksys
Departamento de Física, Universidade da Paraiba, 58051-970, Paraiba, Brazil

A. Ohsawa
Institute for Cosmic Ray Research, University of Tokyo, Tokyo 188, Japan
(Received 2 March 1995)

We present a useful clue to estimate the energy and chemical composition of the primary cosmic radiation between 10^{14} and 10^{17} eV. The method uses various kinds of quantities as measure by a hybrid detector, an emulsion chamber in the central part of an extensive air shower (EAS) array at mountain altitude. The characteristic features needed for the analysis are derived in detail through the Monte Carlo method. The procedure permits an analysis on individual events; it gives an estimation of the mass and energy of a primary nucleus initiating a shower. The estimation of the primary energy is with quite negligible ambiguity. We show that the EAS size measurement could be complementary to quantities as measured by an emulsion chamber detector to improve the accuracy of the primary cosmic ray identification.

PACS number(s): 13.85.Tp, 96.40.De

I. INTRODUCTION

The primary cosmic ray composition plays a crucial role in the knowledge of astrophysics particles, because the primary energy spectrum and also the chemical composition are connected with the problems of the origin and propagation of the cosmic particles into and out of the galaxy.

Direct measurements have been done using balloons, aircraft, and satellites [1–3]. However, these measurements are limited to energies below 10^{14} eV by the low fluxes and the limited exposure time in space or on balloons. Thus, the primary flux composition in the very high energy region (above 10^{14} eV) can be obtained using only indirect methods of ground-based detectors to look at the showers initiated for the interaction of primary nuclei in the upper atmosphere.

There are several air shower parameters that show some sensitivity to the primary composition. However, interpretations of extensive air showers (EAS's) as well as high energy γ-ray families require the knowledge of the properties of nuclear interactions in the energy region above 10^{14} eV. The problem at present is that there are sufficient uncertainties in the mechanism of multiple production of hadrons, especially in the fragmentation region (forward region), because even in accelerators (such as colliders) that have a very high available energy $(0.1–2.0) \times 10^{15}$ eV in the laboratory system, compatible with cosmic ray experiments, only the central region is plentifully observed.

Thus, how to extrapolate the hadronic physics of an accelerator, beyond the kinematics and energy region covered by these machines, implies a corresponding uncertainty in the interpretation of cosmic ray showers. The situation is delicate, because the same shower data can accommodate different and contradictory interpretations.

A new generation of sophisticated air shower detectors, called "hybrid detectors," emulsion chambers in the central part of an extensive air shower array at mountain altitudes, has been developed. The simultaneous observation of high energy γ-ray bundles in the emulsion chamber and accompanying EAS's in large scale can provide details of the primary cosmic ray composition or in principle distinguish groups of nuclei, with an accuracy better than 27%, in the energy region of 10^{15}–10^{17} eV that includes the so-called "knee" region in the primary cosmic ray energy spectrum, as well as the characteristics of hadronic interactions in the extremely high energy region, beyond the collider experiments.

In the last years, experimental data on the small scale of these hybrid detectors became available from three groups: Norikura [4], Tien-Shan [5], and Chacaltaya [6]. They have successfully tested the concept. In this context two large scale experiments are planned: the Omega experiment at Chacaltaya (5200 m above sea level) and the Yangbajing experiment at Tibet (5300 m above sea level). The Omega experiment is an upgrade of the SYS (Saitama, Yamanashi, San Andres) EAS array and Brazil-Japan emulsion chamber.

Furthermore, through correlations between some parameters in which features of high energy γ-ray bundles are related with their associated extensive air shower size, it is possible to get the global characteristics of the primary cosmic ray chemical composition. As already indicated above, a γ-ray family as well as its associated EAS reflects the physics of the particle interaction and primary composition, or in other words, they are sensitive to the hadronic model. However, this sensitivity decreases when the fluctuations in various measurable parameters that reflect fluctuations in shower development are considered. The same global analysis on the basis of some shower parameters for two assumed different models, in spite of some differences, can have an overlapping region.

Thus, an analysis of individual showers using together different measurable parameters to derive other indirectly measurable parameters is a less dependent model than a global analysis of showers on the basis of a measurable parameter.

In this work an analysis on individual events is carried out. It gives an estimation of the energy and mass number of a primary nucleus, on the basis of a formal argument that permits one to construct the joint probability of finding observable quantities with prescribed values. The various kinds of quantities (average values and variances) needed for the analysis were computed through an extensive Monte Carlo simulation using a hybrid code composed of a superposition model to describe the number of interacting nucleon-nucleon pairs implicit in the nucleus-nucleus collision, together with a "ln s" extrapolation of a model on the basis of accelerator data (UA5 algorithm) to describe the hadronic interaction.

The aim of this paper is to examine the accuracy of the method, independent of the model used, to describe the nuclear collision and the possibility of extending the method to practical use in cosmic ray experiments.

II. EXPERIMENTAL CHARACTERISTIC OF γ-RAY FAMILIES AND THEIR ASSOCIATED EAS

The observation stations at mountain altitudes have around 540 g/cm^2 or more of atmospheric depth and the depth is much larger than the mean free path of the nuclear interaction and also the electromagnetic cascade process. Thus, we should expect that an atmospheric shower (high energy γ-ray family and their associated EAS's) is a complex result of successive nuclear interactions and of electromagnetic cascade processes.

The superposition of Coulomb scattering of an electron by atomic nuclei of the matter traversed is called multiple scattering, and it is the main cause of the lateral diffusion of particles in an electromagnetic cascade shower. After the passage of matter at a depth t measured in cascade units, an electron with energy E receives an average angular deflection given as

$$\langle \theta^2 \rangle = \left(\frac{E_s}{E} \right)^2 t, \tag{1}$$

where E_s is the quantity called the scattering constant: 21 MeV. In this way, the lateral spread of an electron (also a γ ray) with energy E from the shower center is estimated as

$$r \sim \frac{E_s}{E} t. \tag{2}$$

Thus, the differences between a γ-ray family and its associated extensive air shower depend mainly on the method of observation. The EAS experiment detects all arriving particles, most of which are electrons and photons with energy around or greater than the critical energy in air, $\sim$ 80 MeV, while the emulsion chamber experiment observes electrons and photons with energy greater than $\sim$ 1 TeV. This difference of their detection threshold energy $\sim 10^4$ makes the lateral spread of the family much smaller than that of EAS's, i.e., around a few cm in the emulsion chamber compared to a few hundred meters in the air shower case. At the same time, the total number of observed particles in the emulsion chamber is $\sim 10^4$ times less than that of an extensive air shower.

A. Emulsion chamber as shower detector

Following the ordinary point of view on hadronic interaction of cosmic ray particles with atmospheric nuclei and subsequent atmospheric propagation, high energy secondary particles are registered as small showers in an emulsion chamber (spot darkness in x-ray films) [7,8]. The shower that starts in the first layers of the chamber is of electromagnetic origin (abbreviated as "γ ray"); on the other hand, a shower starting in deep layers is of nonelectromagnetic origin (abbreviated as "hadron"). These hadron-induced showers can be mainly initiated by a charged pion or nucleon.

As for the detection of the shower efficiency in the emulsion chamber, the most adequate measurable quantities are the shower energy of electromagnetic origin ("γ ray"), E_γ, together with the relative position in the chamber R_γ, defined as the radial distance from the energy-weighted center of the family. Thus, the total electromagnetic energy $\sum E_\gamma$, the mean lateral spread defined as $\sum E_\gamma R_\gamma / \sum E_\gamma$, as well as of course the multiplicity, defined as the numbers of electromagnetic particles (γ rays), N_γ, with energies above an energy threshold are good parameters to characterize the " γ-ray" family.

B. Extensive air shower as detector

The highest energy region of cosmic rays has been studied by the observation of extensive air showers with a ground-based apparatus covering a large area. As already indicated above, the EAS array measures particles, mainly electrons and photons of low energy ($E \sim 80$ MeV), produced in the atmosphere through the arrival of a single primary particle of extremely high energy. Here, the observed particles are the results of the repetition of a number of atmospheric processes.

The mean quantities as measured by an EAS array are

the shower density, defined as the number of particles observed per unit area, and the arrival time distribution of the particles, especially in the near core region, as well as the lateral distribution of the particles. From these one can find such basic quantities as the shower size N_e defined as the total number of particles, and the shower age s which measures the degree of shower development, as well as the atmospheric depth penetrated by the shower at a maximum shower size $X_{\max}$.

III. MAIN ASSUMPTIONS

A. Model of hadronic interaction

The understanding of high energy strong interactions has been improved considerably during the last decade, mainly due to the collider experiments at CERN and Fermilab. However, a typical collider detector will register 80–90% of all secondary particles, but these will only carry 10–30% of the total energy, because the highest energy particles are emitted along the beam pipe and are not detected. This blind spot where the highest energy secondaries occur (called a fragmentation region) leads to uncertainties in the knowledge of nuclear collisions which is crucial to the analysis of cosmic ray phenomena, as happens to the behavior of inelasticity of the hadronic collision in the high energy region which is connected to the validity of the scaling law in this region. That is to say, the inclusive cross section $1/\sigma_{\text{ine}}\, d\sigma_{\text{ine}}/dx$ depends indirectly on the primary energy only through the parameter x, $x = E/E_0$, where E and E_0 are the energies of the secondary and primary particles, respectively, and σ_{ine} is the inelastic cross section.

The problem of the scaling validity in the fragmentation region was investigated by the UA-7 experiment [9], installing a silicon detector in Roman pots at CERN reached at the Interacting Storage Rings (ISR) energies up to $\sqrt{s} = 630$ GeV, and they concluded that it holds in terms of $d\sigma/dy$. While in terms of $1/(\sigma_{\text{ine}})d\sigma_{\text{ine}}/dy$ it indicates scale breaking because the data from the ISR and UA-7 experiments must be divided on different values σ_{ine}, which are distinguished by a factor of 2. A reanalysis made in [10] shows that the degree of violation of the scaling law is not strong in this region; in this case the inelasticity decreases slowly from $K = 0.5$ at $\sqrt{s} = 53$ GeV to (extrapolated value) $K \sim 0.4$ at $\sqrt{s} \sim 1.8 \times 10^3$ GeV.

Despite the uncertainties in the fragmentation region (which must be included in the primary mass resolution), the hadronic interaction implicit in the nucleus-nucleus collision has been simulated with an "ln s" extrapolation of a model on the basis of accelerator data, the UA5 algorithm, reported by the UA5 Group [11], which has two parts, a GENCL code for no diffractive interaction and a DIFFR code for a single diffractive interaction, and reproduced $p\bar{p}$ collisions at $\sqrt{s} = 540$–900 GeV as is reported in the original paper [11].

The asymptotic form ln(s) used in this work is a reasonable alternative for our objectives; once more, the inclusive cross section in $p\bar{p}$ collisions continues to increase rapidly with $\sqrt{s}$ from 23 to 1800 GeV as shown by Abe *et al.* [12], as well as that the previously observed flattening in the shape of the p_t distribution with energy continues up to $\sqrt{s} = 1800$ GeV. As indicated above, an individual analysis using together different measurable parameters of air showers is a less dependent model than a global analysis on the basis of only one measurable parameter.

B. Nuclear effect

In the last several years, experimental data on high energy heavy ion experiments have become available through experiments at CERN, Fermilab, and BNL, as well as through cosmic rays. We try to reproduce nucleus-nucleus collisions by carrying out a Monte Carlo simulation on the basis of these results. The code consists of the following processes: attainment of the number of intranuclear interacting nucleons in a nucleus-nucleus collision, accounting for nuclear fragmentation processes (see the Appendix), and, as already mentioned above, an "ln s" extrapolation of a model on the basis of collider data to describe hadronic collisions.

It has been well established that the superposition principle for nucleus-nucleus collisions is not valid strictly but represents a good approximation, especially for nucleus-air collisions. In this work the number of wounded nucleons is generated through relation (10) (see the Appendix), which includes fluctuations in the fragmentation process, the emission of α particles, evaporated (or free) nucleons, etc. The results obtained with this framework are a little different from the results obtained from the Glauber formalism as reported in [21] where a comparison with experimental results is also carried out.

Fluctuations beyond these values (even if they are large) have very little influence on air shower development, though, because all nucleons will interact in the atmosphere sooner or later. Quantities such as the multiplicity of secondary particles, electromagnetic inelasticity, etc., should therefore be related to the participating nucleons only, whereas spectator nucleons should be disregarded (see Sec. VI for extra fluctuations).

For practical calculations of atmospheric propagation, the cross section σ_{inel} is transformed into collision mean free path, in the atmosphere λ_{air}; for instance, the mean free path for nucleons in the atmosphere is carried out by the formula

$$\lambda_{\text{air}} = 760\sigma_{\text{inel}}^{-0.63}\ \text{g/cm}^2, \tag{3}$$

where σ_{inel} is the inelastic cross section for hadron-nucleon collisions and we used a Hillas's parametrization [13] for the energy dependence of the inelastic cross section:

$$\sigma_{\text{inel}} = \sigma_0[1 + 0.0273\epsilon + 0.01\epsilon^2\Theta(\epsilon)]\ \text{mb}\ , \tag{4}$$

with $\epsilon = \ln(\frac{E}{200\text{GeV}})$, $\sigma_0 = 32.2$ for nucleon-nucleon collisions, $\sigma_0 = 20.3$ for pion-nucleon collisions, and $\Theta(\epsilon)$ is the step function.

Figure 1 summarizes the energy dependence of inelastic cross section for $p\bar{p}$ collision used in this work.

The following bias sources introduced by experimental constraints in the emulsion chamber are taken into account: (a) The error of energy estimation is Gaussian-type as

$$f(x)dx = \exp(-x^2/2\sigma^2)dx, \quad (5)$$

with $x = dE/E$ and $\sigma = 0.12E^{0.19}$; (b) the typical threshold energy $E_{\rm th}$ for E_γ is around 1–2 TeV. However, in this work all calculations are made as a function of $E_{\rm th}$, and only those γ rays inside a radius of 15 cm from the family center are considered.

IV. SENSITIVITY TO PRIMARY MASS COMPOSITION

In order to examine the sensitivity to the primary mass composition of quantities measured as a hybrid detector we provide a direct test of the primary mass resolution of correlations between observed quantities dispersed around the averages with the primary energy.

The dispersion $\sum E_\gamma/E_{\rm th}$, N_γ, and $\sum E_\gamma R_\gamma/\sum E_\gamma$ around the average values are plotted as a function of primary energy and shown in Figs. 1–3 for two extreme cases: proton and iron, as primary particles. The average values of these quantities plotted as a function of the primary energy and for several values of primary mass are shown in Figs. 4–6 respectively.

From these figures we can see that the correlations of the mean values of these quantities with the primary energy (above 50 TeV) are closed with power functions, and present a sufficient primary mass resolution. So a careful analysis extracts information on composition or, in other words, identifies the incident nucleus that generates the individual shower.

On the other hand, hybrid experiments have shown that it is possible to find correlations between quantities observed in the emulsion chamber with their associated EAS's of size N_e. In this work, N_e is traced via the Monte Carlo method, down until their particle energies fall below 0.1 TeV and from this point down by an analytical calculation based on electromagnetic cascade theory using the approximation B [14].

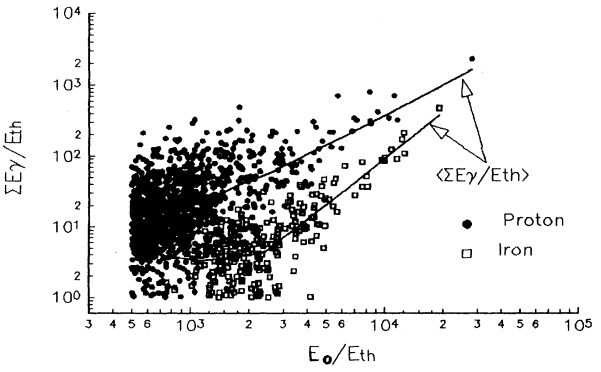

FIG. 1. Scatter plot between the family energy $\sum E_\gamma/E_{\rm th}$ and the primary energy $E_0/E_{\rm th}$. Solid circles are for the proton as the primary particle and squares are for iron as the primary particle. Solid lines represent average values.

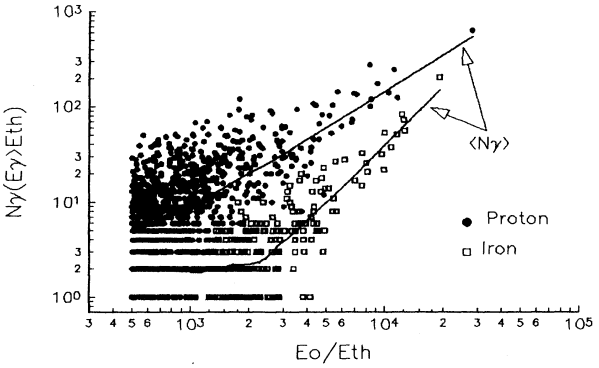

FIG. 2. Scatter plot between the family multiplicity N_γ and the primary energy $E_0/E_{\rm th}$. The symbols are the same as in Fig. 1.

It has been well established that the air shower size N_e is a very stable estimator with a quite negligible ambiguity of the primary cosmic ray energy on the observational level, as far as we are concerned, the mountain experiment, and related as

$$E_0 = a \times N_e \quad (\text{GeV}), \quad (6)$$

with $a \sim 2.0$–2.5; this factor weakly depends on E_0 and is almost independent of the nuclear collision model [15,4]. Shower size is also practically independent of the primary cosmic ray composition. This important characteristic can be observed through Fig. 7(a) and Fig. 7(b) where the correlation between primary energy and shower size is shown under the assumption of proton "normal" composition ($P = 42\%$, $\alpha = 17\%$, CNO=14%, $H = 14\%$, $VH = 13\%$) and heavy dominant composition ($P = 14\%$, $\alpha = 8\%$, CNO= 17%, $H = 14\%$, $VH = 47\%$), respectively, in the primary flux.

Our calculations are in agreement with other independent calculations, for instance, Saito's paper [4]. The few

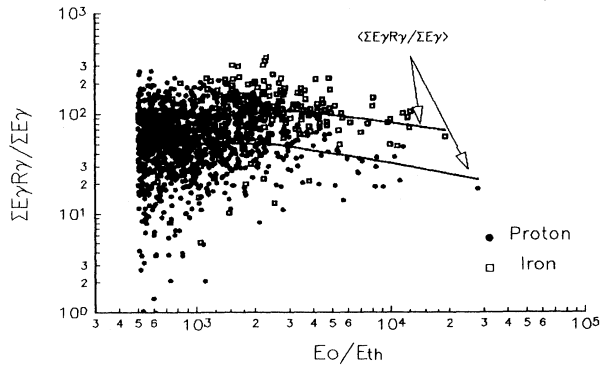

FIG. 3. Scatter plot between the family lateral spread $\sum E_\gamma R_\gamma/\sum E_\gamma$ and the primary energy $E_0/E_{\rm th}$. The symbols are the same as in Fig. 1.

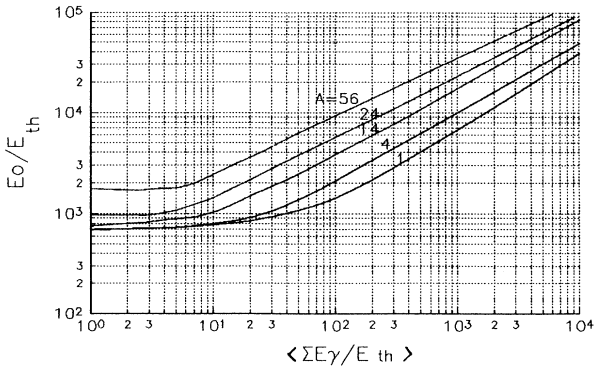

FIG. 4. Average family energy expressed as $\langle \sum E_\gamma / E_{\rm th} \rangle$ vs primary energy. Calculations correspond to different primary nuclei, represented by their mass number.

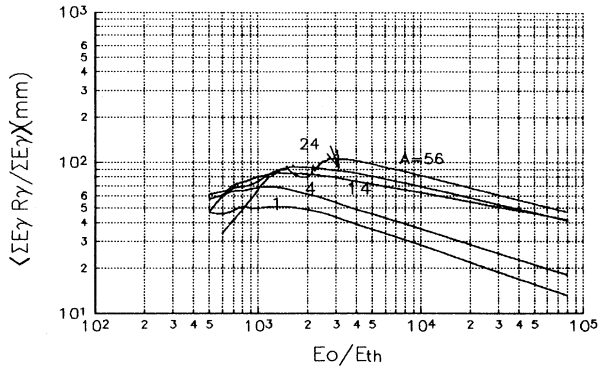

FIG. 6. Average family lateral spread $\langle \sum E_\gamma R_\gamma / \sum E_\gamma \rangle$ vs primary energy. Calculations correspond to different primary nuclei, represented by their mass number.

events with large fluctuations observed in Figs. 7(a) and 7(b) are identified as coming from proton primaries, because some protons can penetrate deep in the atmosphere and even if they have high energies are accompanied by "young" showers with small size (N_e).

It was found that at Chacaltaya the $E_0(\mathrm{GeV})/N_e$ distribution is nearly like the narrow Gaussian with mean 2.0 and standard deviation of 0.25. This characteristic as well as the linear correlation expressed in (6) is a consequence that at mountain altitude the air shower is detected before it enters in the attenuation stage. For instance at Chacaltaya the age shower parameter s is almost independent of the shower size and the average value measured is $\bar{s} = 0.751$–0.823 with a standard deviation between 0.037 and 0.1 in the region of $N_e = 10^5$–10^7 [16] and the shower attenuation happens only to $s > 1$.

In other words, the depth of the shower maximum at these energies is higher in the atmosphere than the Chacaltaya level (5220 m above sea level or 540 g/cm^2 of atmospheric depth). These results are also consistent with measurement by the Fly's Eye detector [17] where the depth of the maximum distribution $X_{\rm max}$ of showers begins only at 500 g/cm^2 of atmospheric depth and their average values $\langle X_{\rm max} \rangle$ increase with the primary energy from $\sim$ 645 g/cm^2 at $10^{-0.5}E$ eV to $\sim$ 770 g/cm^2 at $10^{1.3}E$ eV.

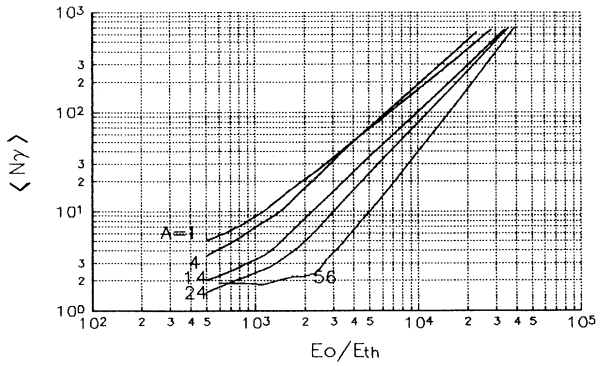

FIG. 5. Average family multiplicity $\langle N_\gamma \rangle$ vs primary energy. Calculations correspond to different primary nuclei, represented by their mass number.

V. ANALYSIS ON INDIVIDUAL SHOWERS

The analysis on individual showers carried out in this work to obtain information on the masses and energies of primary nuclei from observable shower quantities as

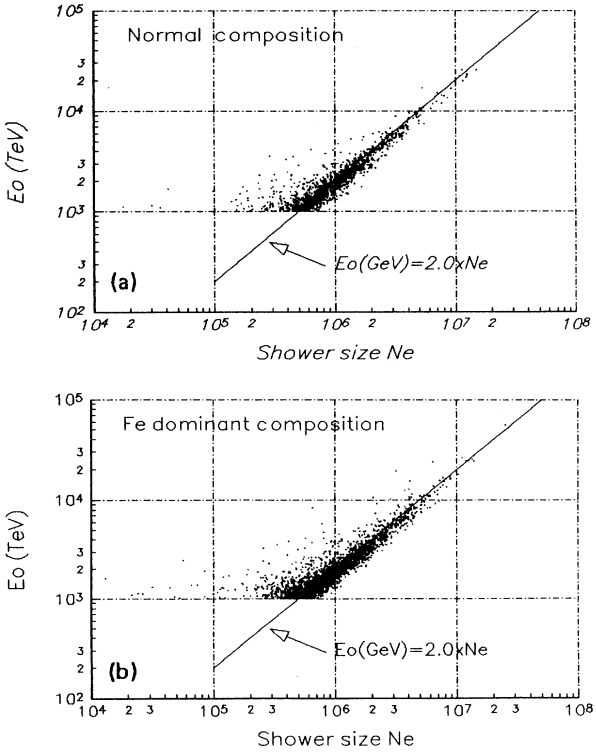

FIG. 7. Correlation between energy E_0, of the primary energy and air shower size N_e, (a) for the case of a "normal" (proton) dominant composition and (b) for the case of an iron dominant composition.

measured by a hybrid detector was developed on the basis of a method reported by Adachi *et al.* [18]. The method is fully used to get a useful clue to the estimation of the energies of γ rays and their production heights, from observable quantities of the electromagnetic cascade as observed by the emulsion chamber.

We make a blow up of this method to the case of primary nuclei initiating showers, even knowing that the stochastic nature of the atmospheric processes smears out the identity of the incident primary particle. However, as already shown in the last section, with Monte Carlo simulations one can derive average quantities and also investigate the fluctuation phenomena.

The method makes it possible to examine the structure of showers starting from some observable parameters. It is, therefore, important because it permits one to derive other parameters which cannot be measured in direct form as primary nuclear mass.

Let the nonobserved quantities, the energy E_0 and the mass number A, of a primary nucleus start a shower. The joint probability

$$P\left(E_0,\ A;\ \sum E_\gamma,\ N_\gamma,\ \sum E_\gamma R_\gamma / \sum E_\gamma\right) \Delta E_0\ \Delta A \tag{7}$$

of finding E_0 and A at prescribed intervals $(E_0 + \Delta E_0)$ and $(A + \Delta A)$, for fixed observed quantities $\sum E_\gamma$, N_γ, and $\sum E_\gamma R_\gamma / \sum E_\gamma$ can be obtained via the Monte Carlo method. For instance at a fixed value of $\sum E_\gamma / E_{\rm th}$ we can scan all possible values of A (mass number) in a determined primary energy region; the same procedure can be made using the other two observable quantities. In this case, an analytical treatment to obtain the joint probability is very hard. Therefore, it can be made graphically, because a function of two variables as $P(E_0,A)$ can be represented by level curves or contour lines.

If the primary nucleus has an energy E_0 and a mass number A, the joint probability $P(E_0,\mathrm{A})$ will have a relative maximum at E_0 and A. Thus, in principle, it is possible to estimate the energy and mass of the primary nucleus.

A further complication is the following: It can happen that as $P(E_0,A)$ is a continuous function, then $P(E_0,A)$ may have several critical points. While every relative maximum occurs at a critical point and consequently the joint probability can have two or most points (E_0,A) where the $P(E_0,A)$ has a relative maximum, in this case, which one is the real point? Probably the higher value of $P(E_0,A)$ is related to the real values of E_0 and A. However, it is not always possible to use this criterion.

There is another way to find the real point (E_0,A) when $P(E_0,A)$ has two or more maxima and it can be achieved

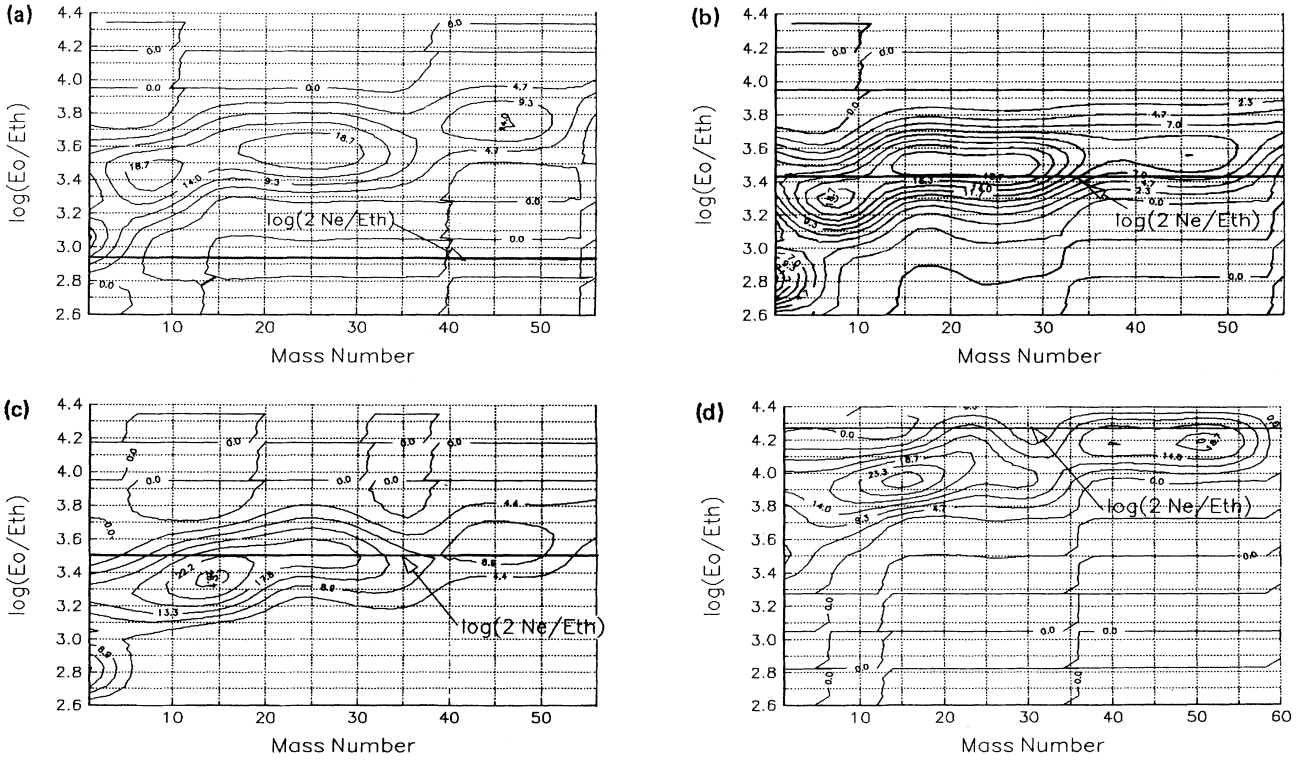

FIG. 8. Relative probability density $P(E_0,\ A)\Delta E_0 \Delta A$. The analysis on simulated events is shown by (a) a shower initiated by a primary nucleus with $E_0/E_{\rm th} = 887$ and $A = 1$, (b) a shower initiated by a primary nucleus with $E_0/E_{\rm th} = 2690$ and $A = 4$, (c) a shower initiated by a primary nucleus with $E_0/E_{\rm th} = 3236$ and $A = 14$, and (d) a shower initiated by a primary nucleus with $E_0/E_{\rm th} = 18\,600$ and $A = 56$. In all the cases the horizontal solid line represents the primary energy estimated from the EAS size as $E_0 = 2.0\ N_e$ (in GeV). Here log represents the natural logarithm.

as follows: The observed quantities as measured by a hybrid detector are $\sum E_\gamma$, N_γ, and $\sum E_\gamma R_\gamma / \sum E_\gamma$, while we also have another observable quantity, that associated with air shower size. As already shown in Sec. IV, N_e is a stable and an almost model-independent estimator of primary energy. Thus, we can choose the maximum point (E_0,A) sufficiently close to E_0 estimated as $E_0 = 2.0N_e$.

To get a better understanding of the situation Figs. 8(a), 8(b), 8(c), and 9(d) show the relative probability density $P(E_0, A)d\Delta E_0 d\Delta A$ at fixed values of $\sum E_\gamma / E_{\rm th}$, N_γ, and $\sum E_\gamma R_\gamma / \sum E_\gamma$ for showers initiated by the proton, α, CNO, and iron, respectively.

VI. ACCURACY IN DETERMINATION OF THE MASS

In order to obtain the accuracy of the above-described method a random selection of 100 simulated events for each type of primaries (proton, helio, CNO, heavy, and iron) was made, corresponding to around 3000 m^2 yr of exposition at Chacaltaya, and one can examine whether shower measurable quantities of the concerned event are consistent with a common origin from a primary nucleus with energy E_0 and mass number A.

Distributions of the difference between $A_{\rm estimated}$ and

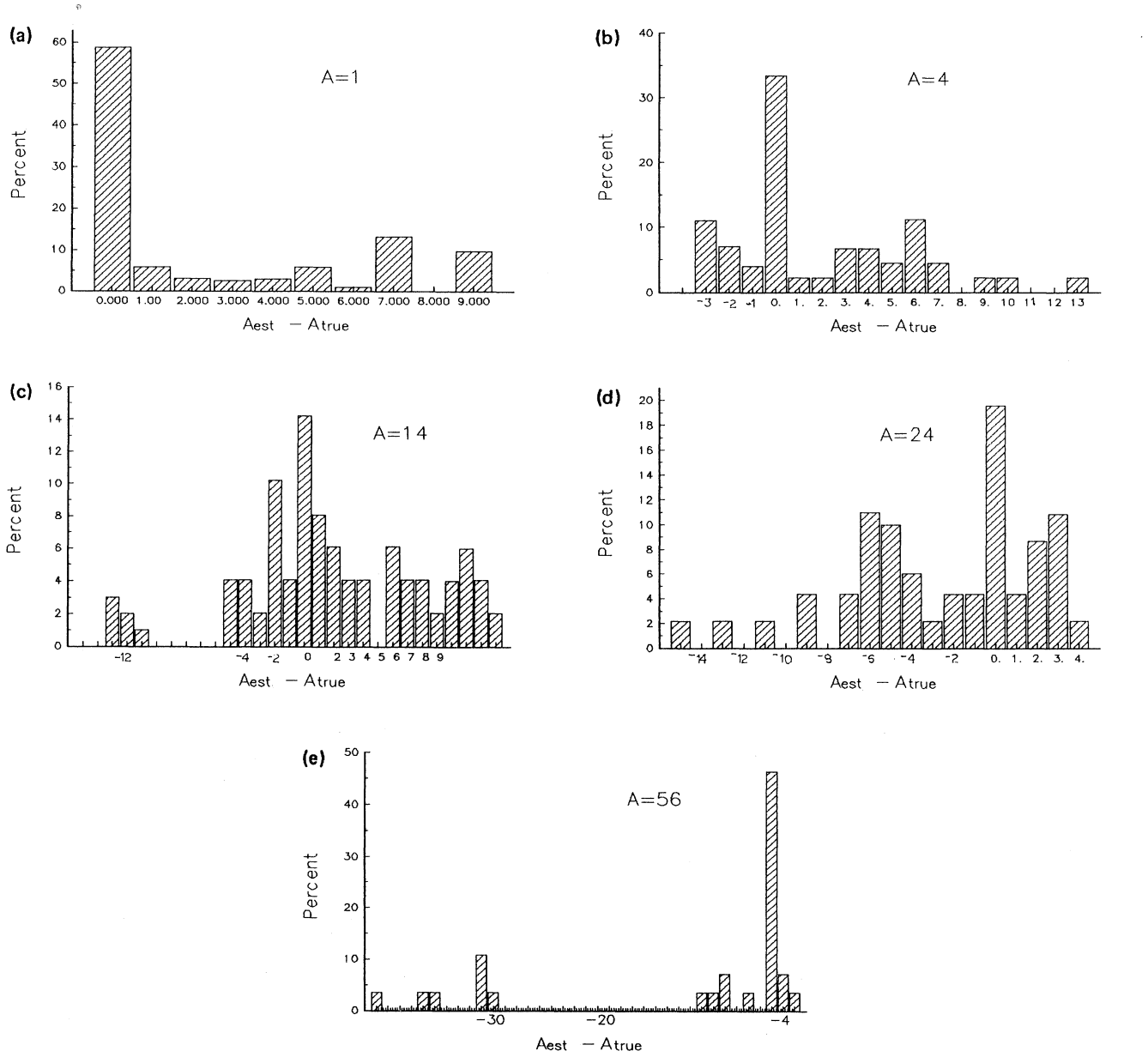

FIG. 9. Distribution of the difference between the estimated mass number $A_{\rm est}$ and the true mass number $A_{\rm true}$. The analysis of simulated events is shown (a) for proton showers, (b) for α showers, (c) for CNO showers, (d) for heavy showers ($A \sim 24$), and (e) for iron showers.

A_{true} are shown in Figs. 9(a), 9(b), 9(c), 9(d), and 9(e) for the five types of nuclei, respectively. The accuracy test carried out from these figures shows that very-light (proton) particles as well as very-heavy particles (iron) initiating showers can be identified with an accuracy better than 45%, while the accuracy by intermediate nuclei identification decreases; we found 34% for α particles, 35% for the CNO group, and 26% for the heavy group, respectively. In short, we estimate the accuracy of the method to primary mass identification better than 36% on average; this value includes 12% of events that were discarded because they presented a high ambiguity in their interpretations.

Using the same procedure as shown above and now used for primary energy resolution, we found that the air shower size is a very good primary energy estimator with an accuracy better than 87%, while the primary energy estimation from joint probability has an accuracy better than 69% on average showing that the present method is reliable.

Furthermore, other kinds of fluctuations especially referent to a nuclear collision in the forward (fragmentation) region, as well as the nuclear target effect, have to be taken into account, to obtain a more accurately mass resolution.

Admitting an uncertainty between a scaling hold and a mild scaling break in the forward region as expressed in Sec. III A, as well as a binomial distribution for the average interacting nucleon (wounded nucleon N_w) distribution with probability $\langle N_w \rangle / N_w \sim 0.5$ where N_w is obtained using the relation (10) of the Appendix, we have found that the joint probability method permits an accuracy better than 27% to the determination of the primary mass.

VII. CONCLUSIONS

In this work we have shown that using a new generation of sophisticated air shower detectors called "hybrid detectors," an emulsion chamber in the central part of an extensive air shower array at mountain altitudes, it is possible that showers can be classified according to the mass of the primary cosmic ray nuclei, in the energy range from 10^{14} to 10^{17} eV.

Shower quantities as measured by a combined experimental apparatus can find a break-through in confronting the difficulties of EAS and emulsion chamber studies because even the dispersion of the observable quantities $\sum E_\gamma / E_{\text{th}}$, N_γ, and $\sum E_\gamma R_\gamma / \sum E_\gamma$ around their average values are great when plotted as function of the primary energy. The correlations between the mean values $\langle \sum E_\gamma / E_{\text{th}} \rangle$, $\langle N_\gamma \rangle$, and $\langle \sum E_\gamma R_\gamma / \sum E_\gamma \rangle$ with the primary energy presents a primary mass resolution big enough to permit an analysis of individual events.

An advantage of this method is that the primary energy can be estimated from two independent modes: (a) from the air shower size N_e and (b) from the joint probability together with the nuclear primary mass. This peculiar characteristic can be used to check the accuracy of the method that uses the joint probability, because it is the same method used for the primary mass estimation. The knowledge of the primary nucleus energy through the shower size N_e is crucial to a useful use of the method, because ambiguities in the interpretations of the joint probability function can be avoided.

On the other hand, in the last section, it was shown that the accuracy of the method to primary mass identification is better than 27% on average; this value is high enough to resolve the discrepancies in primary composition assumptions or, in other words, confirm a dominant proton or iron composition in the primary cosmic ray particles, in the region of 10^{14}–10^{17} eV.

The method can also be adapted for other types of calorimeter, for instance, a tracking module with streamer tubes, installed in the central part of a gigantic EAS array. This new design can amplify the study of the chemical composition of cosmic ray particles above 10^{17} eV.

ACKNOWLEDGMENTS

The authors wish to express their gratitude to the members of the Brazil Japan-Collaboration and SYS (Saitama, Yamanashi, San Andres) Group for encouragement and initial arrangement of the OMEGA Experimente, especially to Dr. M. Tamada for his valuable software support. This work was partially supported by FINEP, CNPq, and FAPESP (Brazilian Government Agencies).

APPENDIX

1. Multiple collision model in nucleus-nucleus interactions

According to the standard Glauber formalism [19], for nucleus-nucleus (AB) collisions, the average number of participating nucleons in the projectile nucleus (wounded nucleons, N_w) is

$$\langle N_w \rangle = A \frac{\sigma_{pB}}{\sigma_{AB}}, \tag{A1}$$

and the mean number of nucleon-nucleon interactions, N_{coll}, in nucleus-nucleus interactions is related as

$$\langle N_{\text{coll}} \rangle = AB \frac{\sigma_{pp}}{\sigma_{AB}}. \tag{A2}$$

A nice analysis of Glauber's formalism is carried out in [20]. They show that (when the target nucleus is nitrogen) despite the fact that the N_{coll} distribution has a width larger than the N_w distribution (at large values of N_{coll}), both distributions have a maximum at one wounded nucleon and both also decrease rapidly, i.e., for peripheral collisions. Thus, if the target nucleus is light or semilight, for practical calculations the N_{coll} distribution can be obtained by the use of N_w distributions, except for very large values of N_{coll}.

In this work the number of participating nucleons in

the projectile nucleus is obtained on the basis of experimental data [21], from both cosmic ray ($\sim$ 1 TeV/nucleon) and machine ($\sim$ 200 GeV/nucleon). According to this scheme, the wounded nucleons is expressed by

$$N_w = A - A' - 4N_\alpha - N_{\text{free}} \tag{A3}$$

for the process

$$A + B = A' + \text{anything} . \tag{A4}$$

The fragmentation probability of the incoming nucleus A in A' (with $A' > 4$) when the target nucleus B is the air (nitrogen or oxygen) nucleus is taken according to a numerical table summarized by Tsao, Silberberg, and Letaw [22] and for the momentum distribution of fragments a model with minimal correlation among nucleon moments proposed by Goldhaber [23] is used, where the distribution function that reproduced experimental data is expressed as

$$g(P_f)dP_f = \exp(-P_f^2/2\sigma^2)dP_f/4\pi\sigma^2, \tag{A5}$$

with

$$\sigma^2 = \sigma_0^2 A'(A - A')/(A - 1), \quad \sigma_0 = 90 \text{ MeV/c}. \tag{A6}$$

The production rate of α particles, N_α, is obtained through the use of a Poisson distribution

$$P(\langle N_\alpha \rangle, N_\alpha) = 1/N_\alpha! \ \ \langle N_\alpha \rangle^{N_\alpha} e^{-\langle N_\alpha \rangle}, \tag{A7}$$

with $\langle N_\alpha \rangle$ given by Freir-Waddington data [24], and for the free nucleon (N_{free}) distribution a function reported by the JACEE Group [25] is used and expressed as

$$f(\chi)d(\chi) = 2\chi d\chi, \tag{A8}$$

with

$$\chi = N_{\text{free}}/(A - A' - 4N_\alpha). \tag{A9}$$

The results obtained within this framework are a little different from the results obtained from the Glauber formalism as reported in [21] where a comparison with experimental results is also carried out.

[1] N.L. Grigorov, Yu.V. Gugin, I.D. Rapoport, I.A. Savenko, B.M. Yakovlev, V.V. Akimov, and V.E. Nesterov, in *Proceedings of the 12th International Cosmic Ray Conference*, Hobart, Australia, 1971 (University of Tasmania, Hobart, 1971), Vol. 5, p. 1746; N.L. Grigorov, N.A. Mamontova, I.D. Rapoport, I.A. Savenko, V.V. Akimov, and V.E. Nesterov, *ibid.*, Vol. 5, p. 1752.

[2] JACEE Collaboration, T.H. Burnett, S. Dake, J.H. Derrickson, W.F. Fountain, M. Fuki, J.C. Gregory, T. Hayashi, R. Holynski, J. Iwai, W.V. Jones, A. Jurak, J.J. Lord, O. Miyamura, H. Oda, T. Tabuki, Y. Takahashi, T. Tominaga, J.W. Watts, J.P. Wefel, B. Wilczynska, H. Wilczynski, R.J. Wilkes, W. Wolter, and B. Wosiek, Astrophys. J. **349**, L25 (1990).

[3] M. Ichimura, M. Kogawa, S. Kuramata, H. Mito, T. Murabayashi, H. Nanjo, T. Nakamura, K. Ohba, T. Ohuchi, T. Ozawa, Y. Yamada, H. Matsutani, Z. Watanabe, E. Kamioka, K. Kirii, M. Kitazawa, T. Kobayashi, A. Mihashi, T. Shibata, K. Shibuta, H. Sugimoto, and K. Nakazawa, Phys. Rev. D **48**, 1949 (1993).

[4] T. Saito, T. Yuda, K. Kasahara, S. Torii, N. Hotta, M. Sakata, and Y. Yamamoto, Astropart. Phys. **1**, 257 (1993).

[5] V.V. Arabkin, S.I. Nicolsky, K.V. Cherdyntseva, and S. Shaolov, in *Proceedings of the 22nd International Cosmic Ray Conference*, Dublin, Ireland, 1991, edited by M. Cawley *et al.* (Dublin Institute for Advanced Studies, Dublin, 1992), Vol. 4, pp. 141, 269, and 273.

[6] N. Kawasumi *et al.*, *Proceedings of the 22nd International Cosmic Ray Conference* [5], Vol. 4, p. 253.

[7] C.M.G. Lattes, Y. Fujimoto, and S. Hasegawa, Phys. Rep. **65**, 151 (1980).

[8] Chacaltaya and Pamir Collaborations, L.T. Baradzei *et al.*, Nucl. Phys. **B370**, 365 (1987).

[9] E. Pare *et al.*, Phys. Lett. B **242**, 531 (1990).

[10] A. Ohsawa, Prog. Theor. Phys. **92**, 1005 (1994).

[11] UA5 Collaboration, Nucl. Phys. **B291**, 445 (1987).

[12] F. Abe *et al.*, Phys. Rev. Lett. **61**, 1819 (1988).

[13] A.H. Hillas, in *Proceedings of the 16th International Cosmic Ray Conference*, Kyoto, Japan, 1979 (Institute for Cosmic Ray Research, Tokyo, 1979), Vol. 13.

[14] B. Rossi and K. Greisen, Rev. Mod. Phys. **13**, 240 (1941).

[15] M. Tamada, J. Phys. G **20**, 487 (1994).

[16] N. Ohta *et al.*, in *Proceedings of the 16th International Cosmic Ray Conference* [13], Vol. 13, p. 177.

[17] T.K. Gaisser *et al.*, Phys. Rev. D **47**, 1919 (1993).

[18] A. Adachi, Y. Fujimoto, N. Ogita, S. Takagi, and A. Ueda, Prog. Theor. Phys. Suppl. **32**, 154 (1964).

[19] R.J. Glauber and G. Matthiae, Nucl. Phys. **B21**, 135 (1970).

[20] J. Engel, T.K. Gaisser, P. Lipari, and T. Stanev, Phys. Rev. D **46**, 5013 (1992).

[21] Y. Niihori, T. Shibata, I. Martin, E. Shibuya, and A. Turtelli, Phys. Rev. D **36**, 783 (1987).

[22] C.H. Tsao, R. Silberberg, and J.R. Letaw, in *Proceedings of the 18th International Cosmic Ray Conference*, Bangalore, India, 1983, edited by N. Durgaprasad *et al.* (TIFR, Bombay, 1983), Vol. 2, p. 294.

[23] A.S. Goldhaber, Phys. Lett. **53B**, 306 (1974).

[24] P.S. Freier and C.J. Waddington, Astrophys. Space Sci. **38**, 419 (1975).

[25] JACEE Collaboration, in *Quark Matter '84*, Proceedings of the Fourth International Conference on Ultrarelativistic Nucleus Nucleus Collision, Helsinki, Finland, 1984, edited by K. Kajantie, Lecture Notes in Physics Vol. 221 (Springer, New York, 1985).